GRAPEVINE RESPONSES TO RED BLOTCH DISEASE – A STRUCTURAL-FUNCTIONAL PERSPECTIVE OF SYMPTOMATOLOGY DEVELOPMENT AND FRUIT QUALITY

Authors: Bhaskar BONDADA[1], Bailey HALLWACHS[1], Marc FUCHS[2], Sadanand DHEKNEY[3], Benham KHATABI[3], Alexander LEVIN[4], Patricia SKINKIS[5]

[1]*Washington State University, Wine Science Center, 2710 Crimson Way, Richland, WA 99354, USA*
[2]*Cornell University, Section of Plant Pathology, Ithaca, NY 14853, USA*
[3]*University of Maryland Eastern Shore Princess Anne, MD 21853, USA*
[4]*Oregon State University, Southern Oregon Research and Extension Center, Central Point, OR 97502, USA*
[5]*Oregon State University, Corvallis, Oregon, 97331, USA*

*Corresponding author:*bbondada@wsu.edu*

Abstract:

Context and purpose of the study - Red Blotch disease caused by *Grapevine red blotch-associated virus* (GRBaV) is a severe concern to grape growers and winemakers in major grape-growing regions worldwide. One key aspect of all viruses, including Red Blotch, is their intimate association with cell components and anomalous structures following infection. Therefore, the objective of this study was to analyze symptomatology, vine function, fruit quality and ultrastructure of various tissues and document the relationship of ultrastructural cytopathology with the GRBaV infection in Pinot Noir and Merlot employing various microscopy techniques. Such knowledge is fundamental to understanding the progression and the mechanisms by which the virus causes the infection, and designing strategies to control its spread in vineyards.

Material and methods – During the growing season, vine samples were collected from vineyards with a history of Red Blotch (Pinot Noir and Merlot) located in the states of Washington and Oregon. Starting at flowering, shoots (leaf and stem tissues) were sampled for microscopy analysis. These samples were used to determine the structure and functionality of the vascular strands (xylem and phloem) using callose-specific dye, aniline blue, and various microscopy techniques. At harvest, fruits were sampled to compare primary and secondary metabolites between healthy and infected vines.

Results – The infected vines exhibited typical red blotches in leaves with pinkish-red-colored veins without rolling off the margins at the onset of ripening. The infected vines developed clusters of hens and chickens and altered seed morphology. Conversely, the healthy seeds were pyriform with a distinct beak. The infection significantly altered the primary and secondary metabolites desired for making wine. Since post-veraison berry development and ripening rely on phloem influx, the altered metabolism was indicative of a disruption of the phloem pathway either in the source leaf or in the berries. While the infected vines maintained the primary leaf anatomical organization, the chloroplast underwent significant ultrastructural changes ranging from the complete dismantling of the chloroplasts to massive accumulation of starch and plastoglobuli development in addition to tannins in the cytoplasm. The study demonstrated that structural integrity is a key to maintaining the normal metabolism of the grapevine, providing new insights into implementing innovative approaches for Red Blotch disease management.

Keywords: Callose, Chloroplast, Grapevine, Plasmodesmata, Red blotch, Sieve tubes, Tylosis, Xylem.

1. Introduction

Grapevine red blotch disease (GRBD) emerged within the past decade, disrupting North American vine stock production and vineyard profitability (Sudarshana et al., 2015). GRBD, first reported in CA in 2008, is caused by Grapevine red blotch virus (GRBV), a putative member of a new genus within the family Geminiviridae and composed of a single-stranded circular DNA genome belonging to the genera *Grablovirus* (Varsani et al., 2017). It infects red and white cultivars; however, the symptomatology varies between them. Typically, the afflicted red cultivars develop red blotches in leaves with pinkish-red-colored veins without any rolling of the margins at the onset of ripening (Golino et al., 2002; Bondada et al., 2019). Conversely, in white cultivars, the mature leaves develop yellowing and marginal necrosis instead of red blotches, rendering the symptoms less apparent (Krenz et al. 2014, Sudarshana et al. 2015). Furthermore, the incidence and severity of the symptoms vary depending on environmental conditions and cultural practices (Sudarshana et al., 2015; Bondada et al., 2019).
Like any other virus, following the infection creates an intimate association with cell components and forms unusual structures and symptoms (Bondada et al., 2019). Accordingly, the management of GRBV depends on the knowledge of the symptomatology of the infection at the whole plant and cellular levels. Symptoms, the purest, most authentic, and the most tangible form of physiological response in advance to a harmful stimulus, mirror the abnormal structure, function, and metabolism (Duan et al., 2022). Therefore, in-depth characterization and fundamental understanding of organs' symptomatology in different plants at the whole plant and cellular levels will help us understand dynamic interactions between the virus and the host (Ray and Casteel, 2022), illuminating how the virus enters the vines, its distribution and survival following entrance throughout the vine, infection cycle, and its strategies to manipulate physiology (Bondada et al., 2019). This crucial information will aid the growers in implementing effective management practices toward minimizing the spread of GRBD. This study attempted to understand the GRBV infection process by examining the symptomatology and various primary and secondary metabolites in berries of healthy and infected vines.

2. Material and methods

Plant material and growing conditions

Plant materials - This study was conducted in Pinot Noir and Merlot vineyards with a history of GRBD located in the states of Washington and Oregon, USA. The Pinot Noir vines, clone 828 grafted onto RG (Riparia galore) rootstock, were head-trained and cane-pruned with vertical shoot positioning catch wires. The Merlot vineyard in Benton City, WA, was own-rooted, and trained onto VSP trellis system (cordon-trained and cane-pruned). Standard cultural practices were employed in both vineyards to manage pests and diseases. Starting at flowering, shoots (leaf and stem tissues) were sampled to determine the structure and functionality of the vascular strands (xylem and phloem) (Bondada, 2014). At harvest, fruits were sampled to compare primary and secondary metabolites between healthy and infected vines.

Statistical analysis - T-tests were used to determine the difference between healthy and infected vines set at an alpha level of $\alpha = 0.05$ using SigmaPlot (version 14.5; SPSS Inc., Chicago, IL).

3. Results and discussion

3.1. Transverse sections through healthy and afflicted canes revealed a brown bark (epidermis) composed of dead epidermis, cortex, and primary phloem (Figure 1) induced by periderm formation from an active phellogen or cork cambium, a lateral meristem that produces the periderm (Esau, 1948; 2014; Stevenson et al., 2005), indicating both canes formed periderm and underwent secondary growth, a developmental process driving radial expansion by forming secondary phloem centrifugally and secondary xylem (woody structures) centripetally (Bondada, 2014) The periderm, which disconnects the primary phloem, including the fiber cap, cortex, and epidermis from internal tissues, typically activates just the interior of the primary phloem (Stevenson et al., 2005) (Figure 1). However, in the infected canes, it developed inside the secondary phloem (Figure 1). Consequently, the layered configuration of phloem tissues consisting of alternating bands of hard and soft phloem was not easily distinguishable in infected canes. Except for this difference, the healthy and infected canes were structurally similar (Figure 1). In both cases, the secondary phloem was made of alternating bands of soft and hard phloem, a signature characteristic of wine grapes (Bondada, 2014). The narrow, dense, hard phloem band consisted of fibers, and the wider soft phloem band consisted of sieve tubes. However, the

conductive sieve tubes, including the fibers, were less developed in the infected canes, probably due to the formation of periderm close to the sieve tube elements (Figure 1). Since the phloem primarily translocates sugars from the source to sink tissues (Lucas et al., 2013), such an anomaly will likely slow the ripening of grape berries by restricting sugar translocation. The primary phloem comprised of parenchymatous tissues bounded by a subepidermal fiber cap was crushed by the periderm (Figure 1). These extraxylary fibers consisted of a cluster of fibers whose cross section resembled a porous kidney-shaped framework with thickened secondary cell walls filling the lumen.

Except for the cell size differences, the cellular organization of canes was similar in healthy and infected vines. In both cases, canes exhibited a highly structurally specialized vascular system marked by possession of secondary phloem tissues, vascular wide rays, large xylem conduits juxtaposed with mechanically robust fiber cells, and periderm outside the phloem in the healthy and within the phloem in infected canes (Figure 1). Among the vascular tissues, the cluster of centripetal secondary xylem vessels embedded in the xylary fibers and separated by radiated bands of parenchyma cells were the most significant structures with thick walls, which were diffuse in distribution (Figure 1); however, the vascular rays dominated the cross-sections. The lumens were open and were clearly visible in both canes. Most lumens of solitary vessels were circular to elliptical (Figure 1), whereas the lumens of radial multiples were neither circular nor elliptical (Figure 1).

Fruit compositional analysis revealed that GRBD infection altered berry physiology and ripening (Table 1). The sugar content was low in the infected berries, whereas their Brix level was high, indicating that infected berries shriveled due to restricted ripening (Table 1). Similar low Brix levels were observed in other wine grapes such as Cabernet Sauvignon and Chardonnay ((Sudarshana et al., 2015). Since berries accumulate potassium just like sugars through phloem translocation (Bondada 2014), its content was also low in the infected berries (Table 1). Furthermore, compared to healthy berries, the infected berries were less acidic due to low titratable acidity ensuing from low contents of tartaric and malic acids, which explains their high pH (Table 1). Cabernet franc infected with GRBD exhibited a similar pattern (Bowen et al., 2020). Conversely, alpha amino compounds and YAN were high in the infected berries. Regarding phenolic compounds, the infected berries maintained anthocyanins, whereas the monomeric (catechin) and polymeric (tannins) flavanols and flavonol (quercetin) were reduced (Table 1). The reduced contents of phenolic compounds in the infected berries reflected an inhibited flavonoid pathway responsible for manufacturing all secondary metabolites.

4. Conclusions

GRBD-infected canes showed activation of cork cambium within the secondary phloem resulting in its partial destruction and functioning of the sieve tube elements. Such disruption inhibited berry ripening by slowing down the sugar accumulation process. Except for the anthocyanins, the phenolic compounds of flavanols and flavonols were reduced in the GRBD-infected berries. This study demonstrated that a comprehensive analysis of the symptomatology of GRBD is needed for designing effective strategies for minimizing the spread of the disease.

5. Acknowledgments

This study was supported by the Northwest Center for Small Fruits Research, a USDA - ARS research-led consortium funded by the USDA.

6. Litterature cited

BONDADA, B. 2014. Structural and compositional characterization of suppression of uniform ripening in grapevine: A paradoxical ripening disorder of drape berries with no known causative clues. Journal of the American Society for Horticultural Science 39, 567–581.

BONDADA B., SKINNER P., FUCHS M., WALKER A. 2019. Protection of grapevines from red blotch by understanding mechanistic basis of its infection (pp. 846-847). Thessaloniki: 21st GiESCO International Meeting: ‘A Multidisciplinary Vision towards Sustainable Viticulture.

BOWEN P. BOGDANOFF C., POOJARI S., USHER K., LOWERY T., ÚRBEZ-TORES J. R., 2020. Effects of Grapevine Red Blotch Disease on Cabernet franc Vine Physiology, Bud Hardiness, and Fruit and Wine Quality. American Journal of Enology and Viticulture 71, 308-318.

DUAN, S., WU Y., ZHANG C., WANG l., SONG S., MA C., ZHANG C., WANG S., BONDADA B., XU W., 2022. Understanding calcium functionality by examining growth characteristics and structural aspects in calcium-deficient grapevine. Scientific Reports 12, 3233. https://doi.org/10.1038/s41598-022-06867-4

ESAU K., 1948. Anatomic effects of the viruses of Pierce's disease and phony peach. Hilgardia 18, 423-482.

GOLINO D., SIM S. T., GILL R., ROWHANI A. 2002. California mealybugs can spread grapevine leafroll disease. California Agriculture 56, 196-201.

KRENZ B., THOMPSON J. R., McLANE H. L., FUCHS M., PERRY K. L. 2014. Grapevine red blotch-associated virus is widespread in the United States. Phytopathology 104, 1232-1240.

LUCAS W. J., GROOVER A., LICHTENBERGER R., FURUTA K., YADAV S. R., HELARIUTTA Y., et al. 2013. The plant vascular system: evolution, development and functions. Journal of Integrative Plant Biology 55, 294–388.

RAY S., CASTEEL C. L., 2022. Effector-mediated plant–virus–vector interactions. The Plant Cell 34, 1514–1531.

STEVENSON J. F., MATTHEWS M. A., ROST T. L., 2005. The developmental anatomy of Pierce's disease symptoms in grapevines: Green islands and matchsticks. Plant Disease 89, 543-548.

SUDARSHANA M. R., PERRY K. L., FUCHS M. F., 2015. Grapevine red blotch-associated virus, an emerging threat to the grapevine industry. Phytopathology 105, 1026–1032.

Table 1. Primary and secondary metabolites as influenced by GRBD infection.

	Healthy	Infected
Brix	22.3 a	24.2 b
Glucose + Fructose (g/L)	223 a	242 b
Sugars (mg/berry)	371 b	281 b
pH	3.20 a	3.40 b
Titratable acidity (g/L)	9.1 a	7.9 a
Malic acid (mg/berry)	7.9 b	4.7 a
Tartaric acid (mg/berry)	9.8 b	6.8 a
Ammonia (mg/L)	97 a	154 b
Alpha ammonia compounds (mg/L)	161 a	270 b
Yeast assimilable nitrogen (mg/L)	240 a	397 b
Potassium (mg/berry)	2.25 b	1.71 a
Catechin (mg/berry)	0.384 b	0.256 a
Quercetin glucosides (µg/berry)	46 b	24 a
Tannins (mg/berry)	0.790 b	0.375 a
Polymeric anthocyanins (mg/L)	7.25 a	8.25 a
Total anthocyanins (mg/berry)	1.15 a	0.95 a
Catechin / tannin index	0.50 a	0.69 b
Polymeric anthocyanins /tannin index	0.015 a	0.026 b

Means within rows followed by the same letter are not significantly different (t-test at $P < 0.05$).

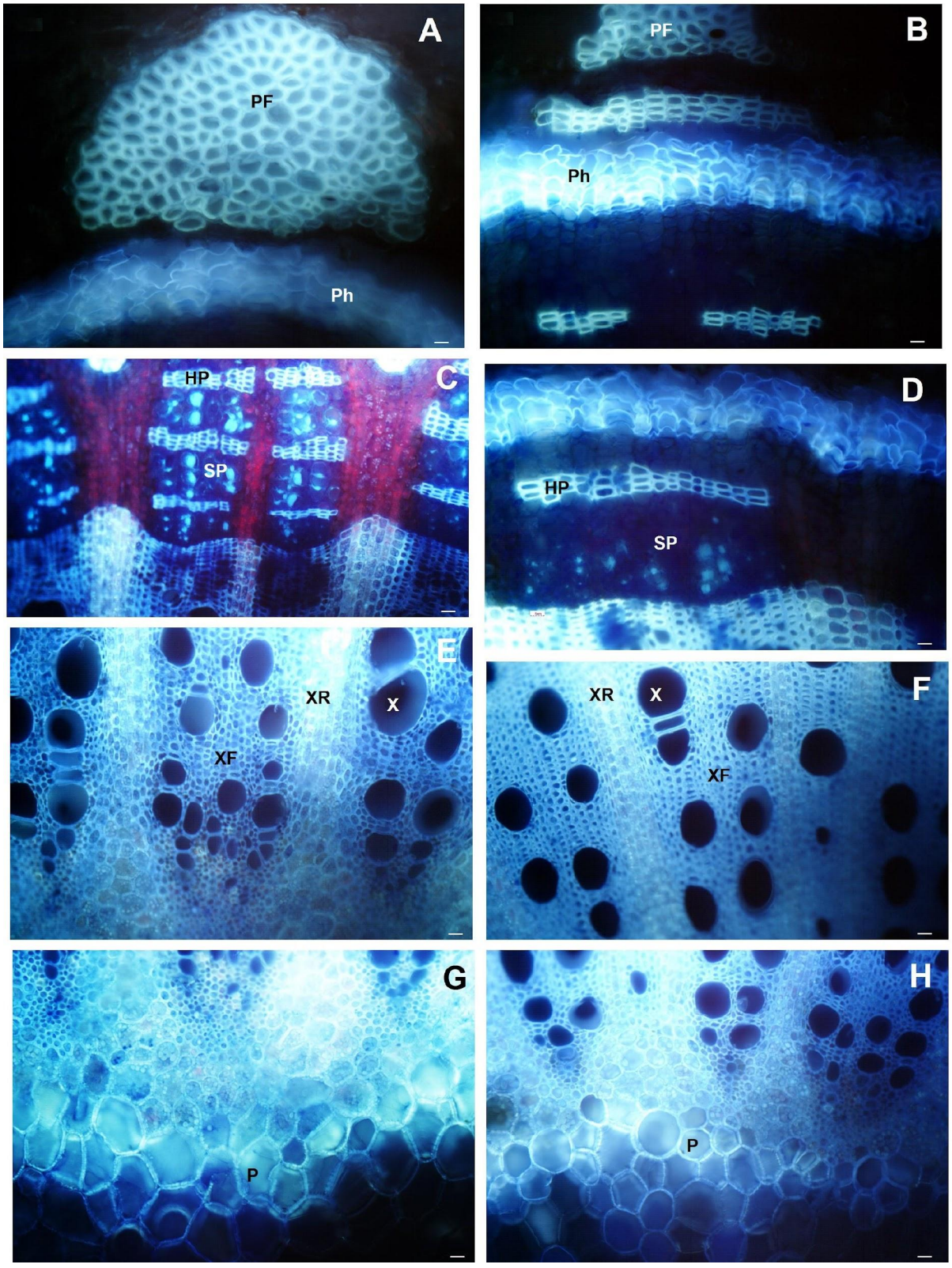

Figure 1. Transverse light micrographs of a (A) healthy and (B) infected cane showing primary phloem fiber cap and phellogen, (C) healthy and (D) infected cane showing secondary phloem, (E) healthy and (F) infected cane showing secondary xylem, (G) healthy and (H) infected cane showing the pith parenchyma cells. Scale bars: 5 µm (A-H). P = Pith; PF = primary phloem fiber; Ph = Phellogen; HP = Hard secondary phloem; SP = Soft secondary phloem; XR = xylem ray parenchyma; XF = xylary fibers; X = xylem vessels.